Analytical Biochemistry 429 (2012) 108–115

Contents lists available at SciVerse ScienceDirect

Analytical Biochemistry

journal homepage: www.elsevier.com/locate/yabio

Highly sensitive and selective hydrogen peroxide biosensor based on hemoglobin immobilized at multiwalled carbon nanotubes–zinc oxide composite electrode

Selvakumar Palanisamy, Srikanth Cheemalapati, Shen-Ming Chen *

Department of Chemical Engineering and Biotechnology, National Taipei University of Technology, Taipei 106, Taiwan, Republic of China

ARTICLE INFO

Article history:
Received 8 May 2012
Received in revised form 29 June 2012
Accepted 3 July 2012
Available online 13 July 2012

Keywords:
MWCNT/ZnO
Electrodeposition
Hemoglobin
Direct electrochemistry
H_2O_2

ABSTRACT

A highly sensitive and selective amperometric hydrogen peroxide (H_2O_2) biosensor based on immobilization of hemoglobin (Hb) at multiwalled carbon nanotubes–zinc oxide (MWCNT/ZnO) composite modified glassy carbon electrode (GCE) is reported. ZnO microsponges were electrochemically grown on MWCNT surface by the simple, cost-effective, green, electrochemical method at room temperature. The MWCNT/ZnO/Hb composite film showed a pair of well-defined, quasi-reversible redox peaks with a formal potential ($E^{o\prime}$) of −0.336 V, characteristic features of heme redox couple of Hb. The electron transfer rate constant (k_s) of immobilized Hb was 1.26 s^{-1}. The developed biosensor showed a very fast response (>2 s) toward H_2O_2 with good sensitivity, wide linear range, and low detection limit of 0.02 μM. The fabricated biosensor showed interesting features, including high selectivity, acceptable stability, good reproducibility, and repeatability along with excellent conductivity, facile electron mobility of MWCNT, and good biocompatibility of ZnO. The fabrication method of this biosensor is simple and effective for determination of H_2O_2 in real samples with quick response, good sensitivity, high selectivity, and acceptable recovery.

Over the past decades, multiwalled carbon nanotubes (MWCNT)[1] has been a promising electrode material that is well known for its fascinating properties such as excellent conductivity, fast electron transfer, high surface area [1], and ability to promote the direct electron transfer between the enzymes and the bare electrodes [2]. Due to the aforementioned interesting properties, MWCNT has been extensively employed in the field of electrochemical biosensors. Specifically, functionalized MWCNT modified surfaces have been widely used for promoting the direct electron transfer of various proteins [3,4], whereby MWCNT has acted as a conduit between the prosthetic group of the proteins and the electrode surface. On the other hand, hydrogen peroxide (H_2O_2) has received considerable attention during recent years because of its fascinating antiseptic and bleaching properties that have produced immense applications in various fields [5]. So far, various methods have been used for H_2O_2 analysis, such as titrimetry [6], photometry [7], chemiluminescence [8], and electrochemical method [9,10]. Among the various methods, electrochemical methods have been playing a crucial role because of their real-time measurements and cost-effective protocols. Due to the high selectivity and specificity for H_2O_2, redox enzymes (horseradish peroxidase, cytochrome *c*, and hemoglobin [Hb])-based biosensors have been extensively employed for sensitive H_2O_2 detection [11–14]. Among these redox enzymes, Hb is an ideal model enzyme used in H_2O_2 biosensors because of its known structure, commercial availability, and relatively higher stability [15]. Moreover, Hb has intrinsic peroxidase-like activity and, thus, could be an appropriate substitute for horseradish peroxidase, specifically for improving the biosensor performance and reducing the fabrication cost.

To enhance the performance features of the biosensor and to efficiently immobilize enzymes onto the electrode surfaces, various nanomaterial matrices have been used. Zinc oxide (ZnO) is well known for its interesting features and has been a promising material with good biocompatibility, high surface activity, and rapid electron communication features [16,17]. These salient features of ZnO are highly advantageous for enzyme-based biosensor applications, and ZnO has been used as a potent matrix for immobilizing redox proteins successfully for efficient H_2O_2 detection [17]. Apart from these interesting aspects of ZnO, great interest has been shown toward the synthesis of MWNT/ZnO composites with interesting morphologies using versatile strategies, including

* Corresponding author. Fax: +886 2270 25238.
E-mail address: smchen78@ms15.hinet.net (S.-M. Chen).

[1] *Abbreviations used:* MWCNT, multiwalled carbon nanotubes; H_2O_2, hydrogen peroxide; Hb, hemoglobin; ZnO, zinc oxide; GCE, glassy carbon electrode; $(ZnNO_3)_2{\cdot}6H_2O$, zinc nitrate hexahydrate; KNO_3, potassium nitrate; PBS, phosphate buffer solution; CV, cyclic voltammetry; SEM, scanning electron microscope; UV–VIS, ultraviolet–visible; RSD, relative standard deviation.

0003-2697/$ - see front matter © 2012 Elsevier Inc. All rights reserved.
http://dx.doi.org/10.1016/j.ab.2012.07.001

hydrothermal [18–21], thermal decomposition [22–25], and electrodeposition [26,27]. Among the various approaches, electrochemical deposition is cost-effective, simple, and eco-friendly. However, only few reports are available for the electrodeposition of ZnO microstructures at low temperature (80 °C) [28–31]. No reports are available in the literature for the room temperature electrodeposition of ZnO microstructures on the MWCNT surface for Hb immobilization. Keeping all of these interesting facts about MWCNT and ZnO in mind, we developed a novel amperometric H_2O_2 biosensor using MWCNT/ZnO composite as a matrix and Hb as the model enzyme for our study.

In this article, we present a simple, eco-friendly, one-step electrochemical approach for the deposition of ZnO microsponges on MWCNT modified glassy carbon electrode (GCE). MWCNT/ZnO microsponges could be a promising platform for Hb because the strong electrostatic interactions between positively charged MWCNT/ZnO composite and negatively charged Hb could retain the bioactivity. The as-fabricated MWCNT/ZnO/Hb composite film exhibits high sensitivity, fast response (>2 s), low detection limit, and high selectivity toward H_2O_2 that are ascribed to the large surface area, good biocompatibility, and synergistic effect of MWCNT and ZnO.

Materials and methods

Chemicals

MWCNT with lengths of 0.1 to 10 μm was obtained from Aldrich. Hb (bovine blood) was purchased from Sigma–Aldrich and used as received without any further purification. Zinc nitrate hexahydrate [$(ZnNO_3)_2{\cdot}6H_2O$, 99% pure] and potassium nitrate (KNO_3) were obtained from Sigma–Aldrich. H_2O_2 (30%) was obtained from Wako Pure Chemical Industries. The supporting electrolyte used for all experiments was phosphate buffer solution (PBS, pH 7.0), which was prepared using 0.05 M Na_2HPO_4 and NaH_2PO_4 solutions. All of the chemicals used in this work were of analytical grade, and all of the solutions were prepared using doubly distilled water.

Apparatus

Electrochemical experiments were carried out using a single-compartment, three-electrode-cell apparatus under N_2 atmosphere (an N_2 tube was kept over the solution during measurement). A computerized electrochemical workstation (CHI 1205) was used for cyclic voltammetry (CV) and amperometric measurements. Surface morphological studies were carried out using a Hitachi S-3000 H scanning electron microscope (SEM). Ultraviolet–visible (UV–VIS) absorption spectra were obtained using a Hitachi U-3300 UV spectrophotometer. Amperometric (*i–t* curve) measurements were performed using a CHI-750A potentiostat with an analytical rotator AFMSRX (Pine Instrument, USA). A conventional three-electrode system was used for the electrochemical experiments, with a modified GCE as the working electrode, a saturated Ag/AgCl as the reference electrode, and a platinum electrode as the auxiliary electrode. All measurements were carried out at ambient conditions.

Preparation of MWCNT/ZnO composite

MWCNT (0.01 g/ml) was dispersed well in dimethylformamide with the aid of sonication for 2 h. The precleaned GCE was used for the fabrication of MWCNT/ZnO composite film. Approximately 8 μl of MWCNT (optimized concentration) was drop-casted on the precleaned GCE and dried in an air oven at 30 °C. The MWCNT modified GCE was shifted to an electrochemical cell containing 0.5 mM $(ZnNO_3)_2{\cdot}6H_2O$ and KNO_3 solution. A total of 30 consecutive cyclic voltammograms were recorded in the potential range of 0 to −1.5 V at a scan rate of 50 mV s^{-1}, resulting in the formation of ZnO microsponges on MWCNT modified GCE. The as-prepared composite modified GCE is denoted as MWCNT/ZnO/GCE hereafter.

Fabrication of MWCNT/ZnO/Hb biosensor

Fresh Hb (0.005 g/ml) solutions were prepared in 0.05 M PBS (pH 7.0) and stored at 4 °C when not in use. To immobilize Hb on the as-prepared MWCNT/ZnO composite modified GCE, approximately 8 μl of Hb was drop-casted and dried at room temperature. We noted that the large surface area and high conductivity of MWCNT, along with the good biocompatibility of ZnO, provides high enzyme absorption. The as-obtained MWCNT/ZnO/Hb composite film modified GCE was gently rinsed a few times with doubly distilled water to remove the loosely bound Hb. The fabricated MWCNT/ZnO/Hb electrode was used for further experiments.

Results and discussion

Electrochemical formation mechanism of MWCNT/ZnO composite

The MWCNT modified GCE was transferred to an electrochemical cell containing 0.5 mM $(ZnNO_3)_2{\cdot}6H_2O$ and KNO_3 solution. It is notable that an N_2 atmosphere was maintained throughout the experiments. A total of 30 consecutive cyclic voltammograms were performed in the potential range between 0 and −1.5 V at a scan rate of 50 mV s^{-1} (see Fig. 1). During the first anodic potential scan, a small anodic hump appears at −0.66 V with an onset potential of −0.83 V, indicating the formation of Zn^{2+} ions [32]. Relatively, no anodic peak was observed at MWCNT/GCE in the same potential window. During the electrochemical deposition process, the positively charged Zn^{2+} ions from the bath solution will be attracted toward the negatively charged MWCNT surface by electrostatic driving force and, thus, got anchored at the MWCNT surface. During the second cathodic potential scan, at a more negative potential (~1 V), the as-dissociated NO_3^- ions will undergo further reduction, forming both NO_2^- ions and oxygen. Meanwhile, the released oxygen should be captured immediately by the anchored Zn^{2+} ions, resulting in the formation of MWCNT/ZnO composite (step 1). As reported previously, ZnO electrochemical deposition can plausibly occur by any one of the following reversible mechanistic pathways [32,33]:

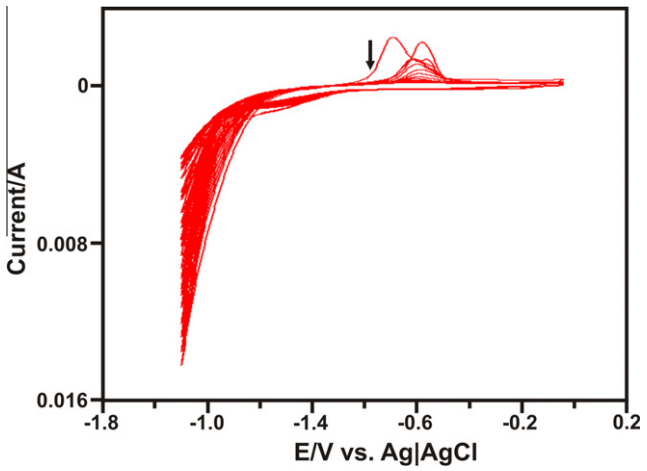

Fig.1. 30 consecutive cyclic voltammograms recorded at an MWCNT modified GCE in 0.5 mM $(ZnNO_3)_2{\cdot}6H_2O$ and 0.5 mM KNO_3 containing N_2-saturated 0.05 M PBS (pH 7.0) at a scan rate of 50 mV s^{-1}.

$$Zn^{2+} + NO_3^- + 2e^- \rightarrow Zno + NO_2^- \quad (1)$$

$$Zn^{2+} + \frac{1}{2}O_2^- + 2e^- \rightarrow ZnO. \quad (2)$$

In our case, because we maintained the N_2 atmosphere during the MWCNT/ZnO electrochemical deposition process, the feasibility of ZnO formation through the association of Zn^{2+} ions and dissolved oxygen as mentioned in Eq. (2) can be neglected. Instead, ZnO formation should have occurred via Eq. (1), where Zn^{2+} ions will associate with the oxygen atoms produced by the reduction of NO_3^- ions.

Surface morphological study

Fig. 2A shows the ZnO microsponges closely anchored on the MWCNT surface. Fig. 2B is the SEM image of the same MWCNT/ZnO composite at lower magnification. The as-grown ZnO structures were between 500 nm and 1 μm in size. The individual ZnO microsponges were interconnected through nanotubes networks. We believe that initially the ZnO growth should have headed along the MWCNT walls because they served as potential templates. Later on, the as-deposited ZnO sponges should have acted as seeds and the growth process might progress laterally, leading to the formation of ZnO microsponges. The large surface area of MWCNT/ZnO composite and the net positive surface charges are helpful for immobilizing negatively charged Hb. SEM results indicated that sponge-like ZnO microstructures have been successfully grown on the MWCNT surface, and the as-prepared MWCNT/ZnO composite material should be a promising platform for the Hb immobilization.

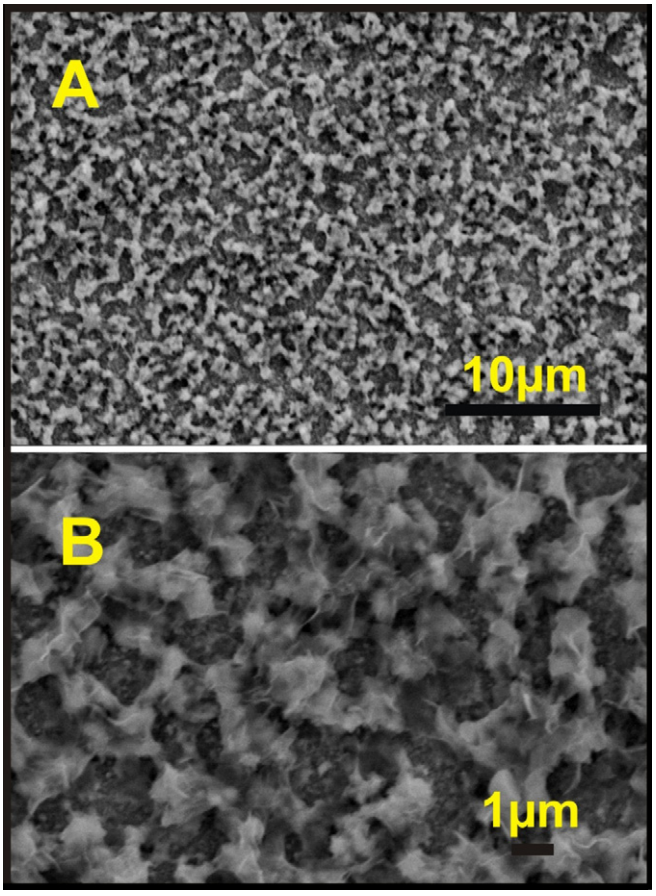

Fig.2. SEM images of electrochemically deposited ZnO microsponges on MWCNT at room temperature (B) and MWCNT/ZnO composite at higher magnification (A).

UV–VIS spectroscopic analysis

The position of the Soret absorption band of heme group may provide information about possible denaturation of proteins [34]. UV–VIS spectroscopy is an important tool that provides valuable information about the possible change of the Soret adsorption band in the heme group region. Therefore, we used UV–VIS spectroscopy as a handy tool to confirm the activity of Hb immobilized on the MWCNT/ZnO composite modified film. As shown in Fig. S1 of the supplementary material, the Soret band of the Hb entrapped in MWCNT/ZnO film was located at 410 nm, similar to that of native Hb [35]. It clearly suggested that no significant denaturation of the immobilized Hb had occurred, revealing the good biocompatibility of the composite matrix.

Direct electrochemistry of Hb

Fig. 3A shows the cyclic voltammograms of different modified GCEs obtained at a scan rate of 0.05 V in PBS (pH 7.0). Cyclic voltammograms were recorded in the potential range of −0.7 to 0.1 V. Bare/GCE does not show any characteristic peaks in this potential window (curve a). Likewise, MWCNT (curve b) and MWCNT/ZnO (curve c) modified electrodes also do not show any characteristic peaks; however, the background current of the latter is higher, clearly indicating that MWCNT/ZnO has higher active electrode area than that of MWCNT. In the same potential, ZnO/Hb and GCE/Hb modified electrodes do not show any characteristic electrochemical signal for Hb (Fig. 3A inset, curves a and b), whereas MWCNT/Hb modified electrode shows a little anodic hump at −0.36 (Fig. 3A inset, curve c). At the MWCNT/ZnO/Hb modified electrode (Fig. 3A, curve d), a pair of well-defined redox peaks appear, indicating that the direct electron transfer of Hb has occurred and it has been augmented in the presence of both MWCNT and ZnO. The formal potential ($E^{\circ\prime}$) calculated from the average of cathodic and anodic peak potentials was −0.336 V (vs. Ag/AgCl). This $E^{\circ\prime}$ value is in close agreement with that of the Hb modified electrode reported previously [36]. The redox peaks were attributed to the electrode process of the electroactive center of Fe(III)/Fe(II) couples in the Hb molecule. The peak potential separation (ΔE_p) was approximately 43 mV, which was smaller than that of other Hb immobilized carbon nanotubes composite films [36,38,39]. Such a small ΔE_p value revealed a fast and quasi-reversible electron transfer process. This result indicates that the synergetic effect of MWCNT/ZnO played a more important role in facilitating the direct electron transfer of Hb than bare/Hb, MWCNT/Hb, and ZnO/Hb modified GCEs. The fast electron transfer of Hb can be attributed to the good biocompatibility, large surface area, and high electronic communication capability of MWCNT/ZnO composite.

Different scan rate studies at MWCNT/ZnO/Hb composite modified electrode

Fig. 3B shows the cyclic voltammograms obtained at MWCNT/ZnO/Hb composite film modified GCE in deoxygenated PBS at different scan rates. On increasing the scan rates, the redox peak currents and peak separation increased linearly. Meanwhile, the cathodic and anodic peak potentials showed a small shift and the peak-to-peak separation also increased. Both anodic and cathodic peak currents increased linearly with scan rates from 100 to 1000 mV s^{-1} (Fig. 3B, inset). In addition, the anodic and cathodic peak potentials shifted toward positive and negative directions, respectively, and it was clear that Hb absorbed onto the MWCNT/ZnO composite matrix underwent a surface-controlled, quasi-reversible process. The electron transfer rate constant (k_s) for Hb at MWCNT/ZnO/Hb composite film modified GCE was calculated using Eq. (3) [37]:

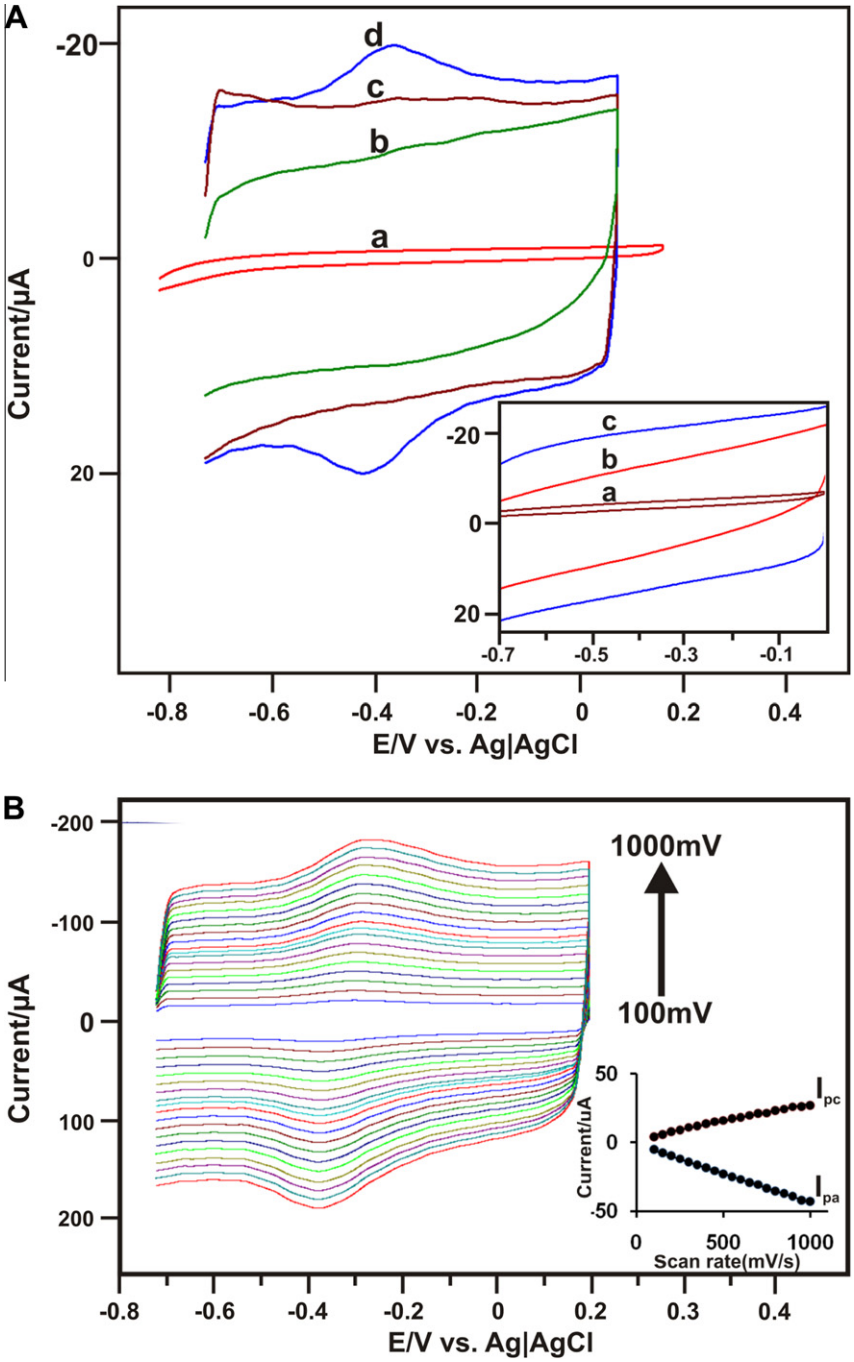

Fig.3. (A) Cyclic voltammograms obtained at bare GCE (a), MWCNT (b), MWCNT/ZnO (c), and MWCNT/ZnO/Hb (d) film modified GCEs in deoxygenated PBS at a scan rate of 50 mV s^{-1}. The inset shows the cyclic voltammograms of MWCNT/Hb (c), ZnO/Hb (b), and GCE/Hb (a) modified electrodes recorded at similar conditions. (B) Cyclic voltammograms recorded at MWCNT/ZnO/Hb composite film modified GCE in deoxygenated PBS at different scan rates. The scan rates from inner to outer are 100 to 1000 mV s^{-1}. The inset shows the linear dependence of I_{pa} and I_{pc} versus scan rates (100–1000 mV).

$$\mathrm{Log}K_s = \alpha\mathrm{Log}(1-\alpha) + (1-\alpha)\mathrm{Log}\alpha - \mathrm{Log}\left(\frac{RT}{nF\nu}\right) - \frac{\alpha(1-\alpha)nF\Delta E_p}{2.3RT}, \quad (3)$$

where R is the gas constant (8.314 J mol^{-1} K^{-1}), T is the room temperature (298.15 K), and ΔE_p is the peak separation of the redox couple. Here, the α value was assumed as 0.5 and the number of electrons transferred was considered as 1. The k_s value at MWCNT/ZnO/Hb composite film was calculated to be 1.22 s^{-1}, and it was higher than the values of Hb immobilized at Nafion-coated, thermally prepared ZnO on MWCNT (1.14 s^{-1}) [36], carbon nanotubes (0.062 s^{-1}) [40], silica-coated gold nanorods (0.83 s^{-1}) [41], and functionalized carbon nanotubes (1.02 s^{-1}) [42]. These results demonstrated that MWCNT/ZnO matrices efficiently facilitated the electron transfer process between Hb and the electrode surface.

Effect of pH

The effect of pH on the electrochemical behavior of MWCNT/ZnO/Hb was investigated as shown in Fig. S2 of the supplementary material. The Hb was found to be electroactive over the tested pH range of 4.0 to 9.0. The $E^{\circ\prime}$ shifted negatively on increasing the pH,

and it exhibited a linear dependence over wide pH range (4.0–9.0) with a slope of −54.1 mV/pH and a correlation coefficient of 0.9837. This slope value was slightly lower than that of the theoretical value of −59 mV/pH at 25 °C for a reversible electron transfer coupled proton transport process [43]. These results also imply that the redox reaction of Hb is a one-proton (H^+) and one-electron (e^-) process. The reaction scheme for the electron transfer process of Hb can be described simply as follows:

$$\text{Hb} - \text{heme Fe(III)} + H^+ + e^- \rightarrow \text{Hb} - \text{heme Fe(II)}. \quad (4)$$

Electrocatalysis of H_2O_2 at MWCNT/ZnO/Hb composite film

The electrocatalytic activity of the MWCNT/ZnO/Hb modified GCE toward H_2O_2 was investigated using CV, and the results are shown in Fig. 4. It is notable that MWCNT/ZnO/Hb composite modified electrode showed a well-defined reduction peak at −0.356 V in the absence of H_2O_2. When H_2O_2 was added into the PBS, a significant increase in the reduction peak at −0.307 V (positive potential shift) was observed, whereas the oxidation peak disappeared, demonstrating the typical electrocatalytic reduction process of H_2O_2. On increasing the H_2O_2 concentrations further, the reduction peak current increased gradually. The maximum reduction peak current was observed for 20.42 μM H_2O_2, where both the increase in peak current and the decrease in overpotential are considered as electrocatalysis. However, in the presence of the same H_2O_2 concentration (20.42 μM), no significant catalytic peak was observed at bare GCE (figure not shown). Relatively, MWCNT/ZnO/Hb modified GCE showed good electrocatalytic property for H_2O_2 reduction. The electrocatalytic response toward the H_2O_2 in linear enslavement could be witnessed between the current response and the concentration of H_2O_2 in the range of 0.01 to 20.42 μM with a correlation coefficient of 0.9981. These results clearly show that MWCNT/ZnO/Hb composite film can be efficiently used for the detection of H_2O_2. The possible mechanism of catalytic reduction of H_2O_2 by Hb could be expressed by the following equations reported previously [44]:

$$\text{Hb}[\text{Heme}(Fe^{III})] + H_2O_2 \rightarrow \text{ComI} + H_2O \quad (5)$$

$$\text{Com I} + H_2O_2 \rightarrow \text{Hb}[\text{Heme}(Fe^{III})] + H_2O + O_2 \quad (6)$$

$$\text{Hb}[\text{Heme}(Fe^{III})] + H^+ + e^- \rightarrow \text{Hb}[\text{Heme}(Fe^{II})] \text{ at electrode} \quad (7)$$

$$\text{Hb}[\text{Heme}(Fe^{II})] + O_2 \rightarrow \text{Hb}[\text{Heme}(Fe^{II})] - O_2 \text{ Fast} \quad (8)$$

$$\text{Hb}[\text{Heme}(Fe^{II})] - O_2 + H^2 + e^- \rightarrow \text{Hb}[\text{Heme}(Fe^{III})] + H_2O_2 \text{ at electrode}. \quad (9)$$

The overall reaction would be

$$H_2O_2 + 2H^+ + 2e^- \rightarrow 2H_2O. \quad (10)$$

Amperometric H_2O_2 reduction studies

In this study, we have used the amperometry technique to evaluate the performance of the developed MWCNT/ZnO/Hb biosensor. During the amperometric *i–t* measurements, the electrode potential was held at −0.34 V (from the CV electrocatalysis) and the N_2-saturated PBS (pH 7.0) was constantly stirred at 1600 rpm. This low applied potential is beneficial for efficient H_2O_2 detection because the matrix effect caused by the common interference species can be minimized and the oxygen reduction current can be limited. For every 50 s, aliquots of H_2O_2 were successively injected into the supporting electrolyte. Fig. 5A shows the amperometric *i–t* response obtained at MWCNT/ZnO/Hb composite rotating disc GCE on various H_2O_2 concentration additions. The response time of the MWCNT/ZnO/Hb composite film toward H_2O_2 was less than 2 s, validating the rapid catalytic reduction process occurring at the composite film surface, which was faster than that of other MWCNT modified Hb-based biosensors (see Table 1), and its overall performance was quite comparable. The response current increased linearly between 0.1 and 36.6 μM H_2O_2 (see Fig. 5A, lower inset). MWCNT/ZnO/Hb composite modified electrode has a sensitivity of 3.63 μA μM^{-1} and a detection limit of 0.02 μM.

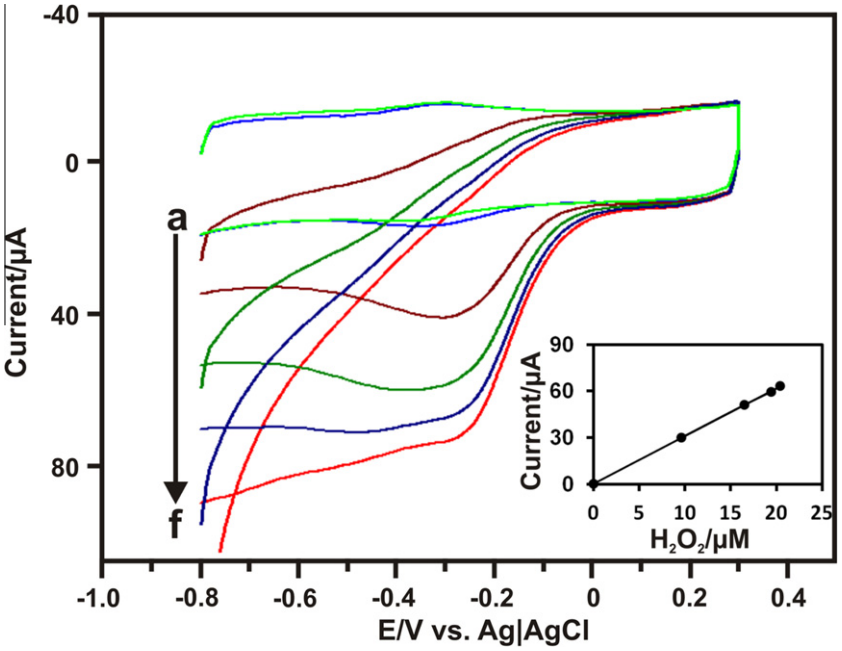

Fig.4. Cyclic voltammograms obtained at MWCNT/ZnO/Hb at a scan rate of 50 mV s^{-1} in the absence (a) and presence of 0.01 μM H_2O_2 (b), 9.62 μM H_2O_2 (c), 16.54 μM H_2O_2 (d), 19.48 μM H_2O_2 (e), and 20.42 μM H_2O_2 (f) in N_2-saturated 0.05 M PBS (pH 7.0). The inset is the plot of cathodic peak current versus $[H_2O_2]$/μM.

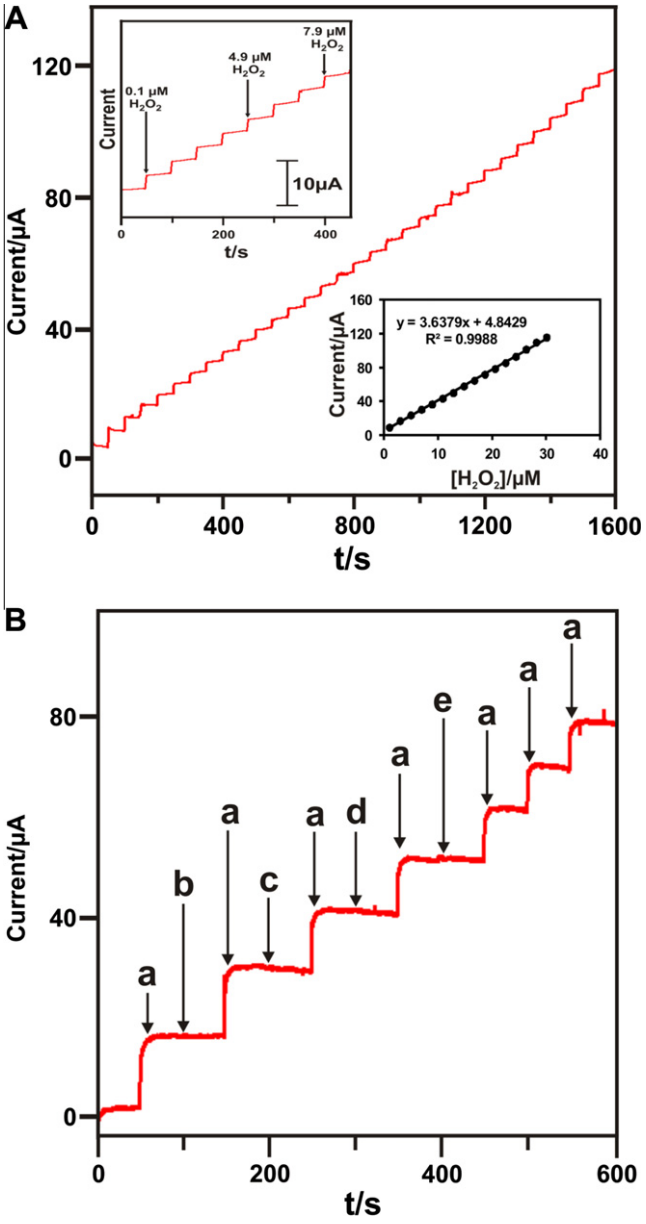

Fig.5. (A) Amperometric *i–t* response at MWCNT/ZnO/Hb composite film modified rotating disc GCE on successive additions of 0.1 to 36.6 μM H_2O_2 into continuously stirred N_2-saturated 0.05 M PBS (pH 7.0). Applied potential = −0.34 V; rotation rate = 1600 rpm. The lower inset is the plot of response current versus $[H_2O_2]$/μM. The upper inset is an enlarged view of the amperometric *i–t* response obtained for 0.1 to 7.9 μM H_2O_2. (B) Amperometric *i–t* response at MWCNT/ZnO/Hb composite film modified rotating disc GCE for the successive addition of 1 μM H_2O_2 (a), 1 mM ascorbic acid (b), 1 mM dopamine (c), 1 mM glucose (d), and 1 mM L-cysteine (e) solutions into continuously stirred N_2-saturated 0.05 M PBS (pH 7.0). Applied potential = −0.34 V; rotation rate = 1600 rpm.

Selectivity, stability, repeatability, and reproducibility studies

The selectivity of the biosensor is very important for its practical applications because H_2O_2 is naturally coexisting with a number of interfering species, including ascorbic acid, dopamine, glucose, and L-cysteine. Therefore, we investigated the selectivity of MWCNT/ZnO/Hb modified electrode in the presence of these common electroactive species. The amperometric technique was employed for evaluating the selectivity of the biosensor. During the amperometric measurements, the supporting electrolyte solution was continuously stirred at 1200 rpm and the electrode potential was held at −0.34 V. Fig. 5B shows the amperometric *i–t* responses obtained at the MWCNT/ZnO/Hb modified electrode for each successive addition of 1 mM ascorbic acid (b), dopamine (c), glucose (d), and L-cysteine (e) at regular intervals (50 s once) into 1 μM H_2O_2 (a) containing N_2-saturated PBS (pH 7.0). It is evident that each addition of the electroactive interfering species brought out a hardly discernible current response, whereas a notable response was observed for 1 μM H_2O_2. The high selectivity of the biosensor is attributed to the fast direct electron transfer rate of Hb at MWCNT/ZnO electrode surface. These results revealed that the prepared H_2O_2 biosensor exhibits high selectivity toward H_2O_2, and it has the ability to reduce the interference from the electroactive species, which is more helpful for practical applications.

To investigate the storage stability of the MWCNT/ZnO/Hb biosensor, the modified electrode was stored in N_2-saturated PBS (pH 7.0) at 4 °C, and its background current was monitored periodically in fresh supporting electrolyte. The modified electrode retained approximately 91.94% and 88.66% of its initial sensitivity after 30 and 60 days, respectively, indicating the excellent storage stability of the composite film. The good biocompatibility of the MWCNT/ZnO composite and the strongly bounded Hb are plausible reasons for the high stability. Moreover, the background current was 92% stable even after 400 consecutive CV potential scanning cycles (conditions same as in Fig. 3A), authenticating the good stability of the composite film. The repeatability and reproducibility of the proposed biosensors were evaluated by CV studies. The other experimental conditions are the same as those described above (see "Electrocatalysis of H_2O_2 at MWCNT/ZnO/Hb composite film" section). The five electrodes fabricated independently showed an acceptable reproducibility with a relative standard deviation (RSD) of 3.57% for each 1 μM H_2O_2 determination. The RSD for each 1 μM H_2O_2 measurements (n = 10) was 1.40%, revealing the good repeatability of the proposed biosensor.

Table 1
Comparison of electroanalytical performance of various Hb-based biosensors.

Film	Sensitivity (μA μM^{-1})	k_s (s^{-1})	Detection limit (μM)	Response time (s)	References
Hb/ZnO–MWCNT/Nafion	0.028	1.14	0.08	3	[36]
Hb/MWCNT	n.a.	0.062	9	7	[40]
ZnO/Nafion/Hb	0.137	3.2	1	n.a.	[44]
Graphene/ZnO/Hb	2.261	1.0	0.6	>10	[45]
MWCNT/ZnO/Hb	3.66	1.22	0.02	>2	This work

n.a.: Not available.

Real sample analysis

The feasibility of MWCNT/ZnO/Hb film for practical application was investigated through real sample analysis by the amperometric *i–t* technique. Commercially available contact lens cleaning solution was used for real sample analysis and was purchased from China Chemical and Pharmaceutical (Taipei). This real sample contains approximately 3% of H_2O_2, and further dilutions were made using PBS (pH 7.0). All of the detected H_2O_2 concentrations were in the linear response range. As can be seen from the calibration plot displayed in Fig. 6, the results obtained using the biosensor are compared with those obtained using the classical potassium permanganate titration method. The results are in good agreement with each other, revealing the good practicality of our method. The real sample analysis results validate that the proposed biosensor can be employed for other real-time sensing applications.

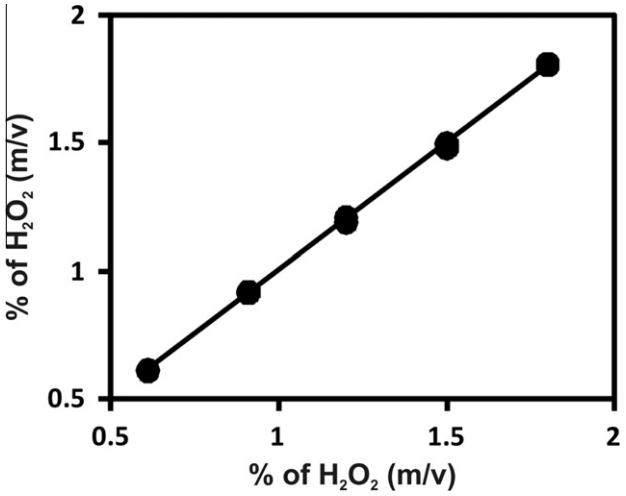

Fig.6. Correlation between the results obtained from the real sample analysis of the Hb biosensor and those obtained with the standard potassium permanganate titration method. *x* axis: enzyme electrode; *y* axis: standard potassium permanganate titration method.

Conclusions

We have reported the facile, green, cost-effective approach for the room temperature electrochemical deposition of ZnO microsponges on the MWCNT surface. SEM results clearly revealed that ZnO microsponges are well formed on the MWCNT surface and are interconnected via nanotubes networks. Along with the unique properties of MWCNT/ZnO microsponges, including good biocompatibility, they were demonstrated to be a good immobilization matrix for Hb. The as-prepared biosensor has good direct electron transfer with the electrode, which may lead to high sensitivity, stability, and selectivity. The fabricated biosensor shows good linear range, fast response, and low detection limit toward H_2O_2. The new cost-effective methodology described here can be applied to develop other MWCNT/ZnO-based enzymatic biosensors. In addition, the MWCNT/ZnO composites can be a promising platform for the fabrication of super-capacitors and solar cells at low cost.

Acknowledgments

This work was supported by the National Science Council and the Ministry of Education of Taiwan (Republic of China). We are very thankful to Arun Prakash Periasamy for his timely help and valuable suggestions.

Appendix A. Supplementary data

Supplementary data associated with this article can be found, in the online version, at http://dx.doi.org/10.1016/j.ab.2012.07.001.

References

[1] O. Akhavan, R. Azimirad, S. Safa, Functionalized carbon nanotubes in ZnO thin films for photoinactivation of bacteria, Mater. Chem. Phys. 130 (2011) 598–602.
[2] N.C. Foulds, C.R. Lowe, Immobilization of glucose oxidase in ferrocene-modified pyrrole polymers, Anal. Chem. 60 (1988) 2473–2478.
[3] J.W. Shie, U. Yogeswaran, S.M. Chen, Haemoglobin immobilized on Nafion modified multi-walled carbon nanotubes for O_2, H_2O_2, and CCl_3COOH sensors, Talanta 78 (2009) 896–902.
[4] Y.P. Sun, K. Fu, Y. Lin, W. Huang, Functionalized carbon nanotubes: properties and applications, Acc. Chem. Res. 35 (2002) 1096–1104.
[5] W. Zhao, H. Wang, X. Qin, X. Wang, Z. Zhao, Z. Miao, L. Chen, M. Shan, Y. Fang, Q. Chen, A novel nonenzymatic hydrogen peroxide sensor based on multi-wall carbon nanotube/silver nanoparticle nanohybrids modified gold electrode, Talanta 80 (2009) 1029–1033.
[6] P.A. Weber, J.E. Thomas, W.M. Skinner, R.S.C. Smart, Improved acid neutralisation capacity assessment of iron carbonates by titration and theoretical calculation, Appl. Geochem. 19 (2004) 687–694.
[7] V.N. Gorala, M.I. Nelena, A.D. Ryabovab, Ferrocene and ferricenium ion as versatile hotometric titrants of H_2O_2 and D-glucose in the presence of peroxidase and glucose oxidase: a ferrocene–peroxidase stairway, Anal. Lett. 28 (1995) 2139–2148.
[8] S. Sakaia, T. Satowa, K. Imakawa, K. Nagaoka, Generation of hydrogen peroxide by a low molecular weight compound in whey of Holstein dairy cows, J. Dairy Res. 75 (2008) 257–261.
[9] J. Hong, Z. Dai, Amperometric biosensor for hydrogen peroxide and nitrite based on hemoglobin immobilized on one dimensional gold nanoparticle, Sens. Actuat. B 140 (2009) 222–226.
[10] S. Liu, Z.H. Dai, H.Y. Chen, H. Ju, Immobilization of hemoglobin on zirconium dioxide nanoparticles for preparation of a novel hydrogen peroxide biosensor, Biosens. Bioelectron. 19 (2004) 963–969.
[11] J. Liu, C. Guo, C.M. Li, Y. Li, Q. Chi, X. Huang, L. Liao, T. Yu, Carbon-decorated ZnO nanowire array: a novel platform for direct electrochemistry of enzymes and biosensing applications, Electrochem. Commun. 11 (2009) 202–205.
[12] Q. Rui, K. Komori, Y. Tian, H. Liu, Y. Luo, Y. Sakai, Electrochemical biosensor for the detection of H_2O_2 from living cancer cells based on ZnO nanosheets, Anal. Chim. Acta 670 (2010) 57–62.
[13] S. Chen, R. Yuan, Y. Chai, L. Zhang, N. Wang, X. Li, Amperometric third-generation hydrogen peroxide biosensor based on the immobilization of hemoglobin on multiwall carbon nanotubes and gold colloidal nanoparticles, Biosens. Bioelectron. 22 (2007) 1268–1274.
[14] C. Guo, F. Hua, C.M. Li, P.K. Shen, Direct electrochemistry of hemoglobin on carbonized titania nanotubes and its application in a sensitive reagentless hydrogen peroxide biosensor, Biosens. Bioelectron. 24 (2008) 819–824.
[15] S. George, H.K. Lee, Direct electrochemistry and electrocatalysis of hemoglobin in Nafion/carbon nanochip film on glassy carbon electrode, J. Phys. Chem. B 113 (2009) 15445–15454.
[16] B.X. Gu, C.X. Xu, G.P. Zhu, S.Q. Liu, L.Y. Chen, M.L. Wang, J.J. Zhu, Layer by layer immobilized horseradish peroxidase on zinc oxide nanorods for biosensing, J. Phys. Chem. B 113 (2009) 6553–6557.
[17] Z. Zhao, W. Lei, X. Zhang, B. Wang, H. Jiang, ZnO-based amperometric enzyme biosensors, Sensors 10 (2010) 1216–1231.
[18] C.L. Kuo, T.J. Kuo, M.H. Huang, Hydrothermal synthesis of ZnO microspheres and hexagonal microrods with sheetlike and platelike nanostructures, J. Phys. Chem. B 109 (2005) 20115–20121.
[19] H. Sun, M. Luo, W. Weng, K. Cheng, P. Du, G. Shen, G. Han, Room-temperature preparation of ZnO nanosheets grown on Si substrates by a seed-layer assisted solution route, Nanotechnology 19 (2008) 125603, http://dx.doi.org/10.1088/0957-4484/19/12/125603.
[20] S. Yamabi, J. Yahiro, S. Iwai, H. Imai, Formation of cellular films consisting of wurtzite-type zinc oxide nanosheets by mediation of phosphate anions, Thin Solid Films 489 (2005) 23–30.
[21] B. Cao, W. Cai, Y. Li, F. Sun, L. Zhang, Ultraviolet-light-emitting ZnO nanosheets prepared by a chemical bath deposition method, Nanotechnology 16 (2005) 1734–1738.
[22] G. Guo, J. Guo, D. Tao, W.C.H. Choy, L. Zhao, W. Qian, Z. Wang, A simple method to prepare multi-walled carbon nanotube/ZnO nanoparticle composites, Appl. Phys. A 89 (2007) 525–528.
[23] A. Rahm, G.W. Yang, M. Lorenz, T. Nobis, J. Lenzner, G. Wagner, M. Grundmann, Two-dimensional ZnO:Al nanosheets and nanowalls obtained by Al_2O_3-assisted carbothermal evaporation, Thin Solid Films 486 (2005) 191–194.
[24] A. Umar, Y.B. Hahn, ZnO nanosheet networks and hexagonal nanodiscs grown on silicon substrate: growth mechanism and structural and optical properties, Nanotechnology 17 (2006) 2174–2180.
[25] G. Deng, A. Ding, W. Cheng, X. Zheng, P. Qiu, Two-dimensional zinc oxide nanostructure, Solid State Commun. 134 (2005) 283–286.
[26] T. Yoshida, D. Komatsu, N. Shimokawa, H. Minoura, Mechanism of cathodic electrodeposition of zinc oxide thin films from aqueous zinc nitrate baths, Thin Solid Films 451 (452) (2004) 166–169.
[27] Y.L. Chen, Z.A. Hu, Y.Q. Chang, H.W. Wang, Z.Y. Zhang, Y.Y. Yang, H.Y. Wu, Zinc oxide/reduced graphene oxide composites and electrochemical capacitance enhanced by homogeneous incorporation of reduced graphene oxide sheets in zinc oxide matrix, J. Phys. Chem. C 115 (2011) 2563–2571.
[28] A.B. Moghaddam, T. Nazari, J. Badraghi, M. Kazemzad, Synthesis of ZnO nanoparticles and electrodeposition of polypyrrole/ZnO nanocomposite film, Int. J. Electrochem. Sci. 4 (2009) 247–257.
[29] A.C. Cruickshank, S.E.R. Tay, B.N. Illy, R.D. Campo, S. Schumann, T.S. Jones, S. Heutz, M.A. McLachlan, D.W. McComb, D.J. Riley, M.P. Ryan, Electrodeposition of ZnO nanostructures on molecular thin films, Chem. Mater. 23 (2011) 3863–3870.
[30] K.N. Han, C.A. Li, M.P.N. Bui, X.H. Pham, G.H. Seong, Control of ZnO morphologies on carbon nanotube electrodes and electrocatalytic characteristics toward hydrazine, Chem. Commun. 47 (2010) 938–940.
[31] G.R. Li, C.R. Dawa, Q. Bu, Z.H. Lu, Z.H. Ke, H.E. Hong, F.L. Zheng, C.Z. Yao, C.K. Liu, Y.X. Tong, Electrochemical growth and control of ZnO dendritic structures, J. Phys. Chem. C 111 (2007) 1919–1923.
[32] M. Izaki, T. Omi, Transparent zinc oxide films prepared by electrochemical reaction, Appl. Phys. Lett. 68 (1996) 2439–2440.
[33] M. Izaki, T. Omi, Electrolyte optimization for cathodic growth of zinc oxide, J. Electrochem. Soc. 143 (1996) L53–L55.

[34] P. George, G. Hanania, A spectrophotometric study of ionizations in methaemoglobin, Biochem. J. 55 (1953) 236–243.
[35] H. Xu, H. Dai, H. Chen, Direct electrochemistry and electrocatalysis of hemoglobin protein entrapped in graphene and chitosan composite film, Talanta 81 (2010) 334–338.
[36] W. Ma, D. Tian, Direct electron transfer and electrocatalysis of hemoglobin in ZnO coated multiwalled carbon nanotubes and Nafion composite matrix, Bioelectrochemistry 78 (2010) 106–112.
[37] Z.Q. Zhai, J. Wu, W. Sun, K. Jiao, Direct electrochemistry of hemoglobin and its electrocatalysis based on a carbon nanotube paste electrode, J. Chin. Chem. Soc. 56 (2009) 561–567.
[38] X. Lu, J. Hu, X. Yao, Z. Wang, J. Li, Composite system based on chitosan and room-temperature ionic liquid: direct electrochemistry and electrocatalysis of hemoglobin, Biomacromolecules 7 (2006) 975–980.
[39] E. Laviron, General expression of the linear potential sweep voltammogram in the case of diffusionless electrochemical systems, J. Electroanal. Chem. 101 (1979) 19–28.
[40] Y.D. Zhao, Y.H. Bi, W.D. Zhang, Q.M. Luo, The interface behavior of hemoglobin at carbon nanotube and the detection for H_2O_2, Talanta 65 (2005) 489–494.
[41] J.J. Zhang, Y.G. Liu, L.P. Jiang, J.J. Zhu, Synthesis, characterizations of silica-coated gold nanorods, and its applications in electroanalysis of hemoglobin, Electrochem. Commun. 10 (2008) 355–358.
[42] R. Zhang, X. Wang, K.K. Shiu, Accelerated direct electrochemistry of hemoglobin based on hemoglobin–carbon nanotube (Hb–CNT) assembly, J. Colloid Interface Sci. 316 (2009) 517–522.
[43] W. Sun, R. Gao, K. Jiao, Electrochemistry and electrocatalysis of hemoglobin in Nafion/nano-$CaCO_3$ film on a new ionic liquid BPPF6 modified carbon paste electrode, J. Phys. Chem. B 111 (2007) 4560–4567.
[44] X. Lu, H. Zhang, Y. Ni, Q. Zhang, J. Chen, Porous nanosheet-based ZnO microspheres for the construction of direct electrochemical biosensors, Biosens. Bioelectron. 24 (2008) 93–98.
[45] J. Xu, C. Liu, Z. Wu, Direct electrochemistry and enhanced electrocatalytic activity of hemoglobin entrapped in graphene and ZnO nanosphere composite film, Microchim. Acta 172 (2011) 425–430.